Analysis of Flow Field and Temperature Distribution in Granary under Novel Ventilation Systems Based on Fractal Structure

Jun Lin[1], KaiXuan Chen[2], Wei Liu[3], Xin Lu*[4]

[*1,2,3,4] School of Energy and Power Engineering, Nanjing university of science and technology, Nanjing, China

[*] Corresponding author; E-mail: luxin@njust.edu.cn

The distribution of velocity and temperature field inside the granary can be used to evaluate ventilation quality. A well-ventilated system with uniform airflow and cooling can effectively prevent moisture accumulation. To address the issue of poor uniformity in ventilation and cooling, this research introduces two new ventilation systems: the non-fractal ventilation system and the fractal ventilation system. The fractal structure was designed based on optimized parameters obtained from rectangular elements with minimum flow resistance. Numerical simulation methods were employed to verify the effectiveness of these ventilation systems. A comparative analysis was conducted, examining the velocity field, temperature field, and velocity uniformity of the two systems. The results demonstrated that the presence of a sand packing zone helped the grain pile zone avoid most of the areas with poor ventilation. The discontinuous pores at the interface between the sand packing zone and the grain pile zone significantly increased flow resistance, effectively reducing the velocity of high-speed ventilation into the grain pile zone and decreasing the permeability of the grain pile zone towards the poorly ventilated areas of the sand pile zone. Furthermore, the fractal structure greatly enhanced ventilation intensity in areas with poor ventilation in the velocity field, while also improving the uniformity of cooling in the temperature field. This research presents an innovative solution for ventilation in room-type warehouses, offering a new option for effective and efficient ventilation.

Key words: *ventilation system; numerical simulation; porous medium packing; fractal structure*

1 Introduction

Every year in China, there is a significant loss of stored grains in granaries, resulting in alarming levels of wastage[1]. In warm and humid environments, grain respiration intensifies, leading to issues such as moisture regain and mildew within the grain pile. Moreover, warm and humid conditions accelerate insect infestation and damage[2]. Experimental research has shown that employing mechanical ventilation to control the temperature and humidity of grain piles effectively reduces grain loss[3], preserves grain quality, and significantly extends the safe storage period.

The design and layout of ventilation pipelines are critical factors in determining the quality of granary ventilation. Traditional two-dimensional planar layouts have evolved into three-dimensional spatial layouts[4] over the years. Spatial layouts allow for faster penetration of the ventilation into the grain pile, resulting in improved cooling rates[5]. However, spatial layouts have not effectively addressed the issue of poor ventilation areas, which can lead to widespread deterioration and spoilage within those regions[6]. To achieve effective ventilation, there is a recommended range for selecting the inlet-air volume for mechanical ventilation [7]. Within this range, a balance can be achieved between cooling rate and energy efficiency. These reference values also apply to spatial layouts. With the same inlet-air volume, spatial ventilation tends to be weaker at the bottom of the granary, leading to larger areas with poor ventilation.

Modern computational fluid dynamics (CFD) has emerged as a powerful tool for addressing the challenge of achieving high-quality ventilation of granary. Thorpe et al. developed a comprehensive numerical model that considers coupled heat and moisture transfer to investigate temperature and airflow variations under different operating conditions in small granaries[5,8], and successfully predicted the performance of a solar granary ventilation drying device[9]. Daniela et al.[10] utilized Thorpe's model to simulate a silo and achieved improved simulation results. As the numerical models for granary continue to advance, they are being incorporated into commercial fluid simulation software, making it convenient for researchers to study granary ventilation simulations. For instance, Olatunde et al.[11] employed FLUENT to examine the influence of different grain pile shapes on ventilation velocity uniformity, while Zhang et al.[12] utilized COMSOL to study the development and movement of the thermal core within a grain pile. In addition, the design of commercial buildings with low cooling load can also be used in granary [13].

Based on the mass transfer equation and Darcy's law, an optimization model for fractal structures in porous medium has been developed. The objective of optimization is typically to minimize entransy dissipation rate or fluid pressure drop. Various optimization models have been proposed, including rectangular unit models[14-15], triangular unit models[16], bionic leaf networks[17], and bionic honeycomb fractal microchannels[18]. The optimized structures can reduce the average mass transfer pressure loss to approximately two-thirds of the maximum mass transfer pressure loss. By reducing pressure losses, the optimized design enhances the overall ventilation efficiency and effectiveness, allowing for stronger infiltration capacity of inlet air in grain.

Research efforts in granaries have mainly focused on improving ventilation and cooling, but there is limited attention given to optimizing ventilation and cooling uniformity. Improving velocity uniformity is crucial for ensuring high-quality ventilation and preventing local moisture accumulation. To address this, a new approach is proposed: elevating the grain pile using sand packing. This research introduces two new ventilation systems: a new type of non-uniform section pipelines wrapped by porous medium (sand) ventilation system (the non-fractal ventilation system) and a new type of non-

uniform section pipelines incorporated with fractal structure wrapped by porous medium (the fractal ventilation system). Using CFD methods, the velocity field and temperature field are studied.

2 Model establishment and condition setting

2.1 Physical model

In this study, the focus is on a room-type warehouse where the physical model consists of the air zone at the top of the granary, the grain pile, and the porous medium ventilation zone, as depicted in Fig.1(a). The dimensions of the established physical model are as follows: length of 38 m, width of 22.86 m, and height of 11.7 m. The height of the packing zone is 1.2 m, and the height of the grain pile reaches 6 m. To ensure symmetrical airflow, the air inlets are arranged longitudinally with 16 inlets on both sides. Pressure outlets are positioned equidistantly with 12 windows located on the front and rear sides of the air layer, as shown in Fig.1(b). The non-uniform section pipeline, illustrated in Fig.2(a), has an inlet diameter of 0.4 m and expands to a diameter of 0.6 m in the middle expansion section. This pipe is longitudinally laid in the sand packing zone beneath the grain pile. On the other hand, the alternative model incorporates a fractal structure within the non-uniform section ventilation pipeline to enhance local area ventilation. The first-level fractal branch pipeline is centrally symmetrical and horizontally connected to the main pipe. Two sets of second-level fractal branches, parallel to the main pipeline, are longitudinally arranged on both sides, connecting to the first-order branch pipe. The specific layout is visualized in Fig.2(b), and detailed parameters can be found in Tab.2.

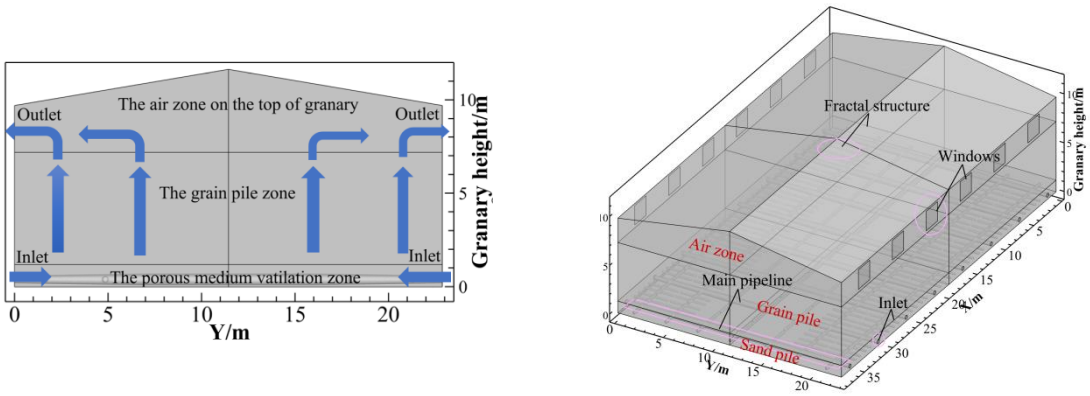

(a) Calculation domain of granary model **(b) 3D drawing of the fractal granary**

Fig.1 Physical model of room-type warehouse

Note: the arrows indicate the direction of air flow

In the grid division for gas-solid coupling problems, the mesh size needs to be larger than the particle size. In this research, the mesh sizes for the porous medium zone and the air zone were all greater than 15 mm and 100 mm, respectively. Unstructured grid division method was used in the porous medium ventilation zone with complex structure and the air zone with irregular volumes. Since the grain pile zone has a uniform structure and regular volumes, so a structured grid division method was employed for this zone. And three groups of grids were used to check the grid and the independence of the results from the selected grid. The number of units in each group of grids was as follows: 0.89 million and 1.26 million (coarse grid), 1.34 million and 1.84 million (medium grid), 1.78 million and 2.32 million (fine grid) for the non-fractal and fractal systems respectively. Three groups

of grids were simulated for 72 hours under same conditions. The results were compared with the medium grids to obtain the differences with the fine and coarse grids. The maximum mean temperature difference between fine and medium mesh, coarse and medium mesh were less than 0.15 K and 0.2 K, respectively. These findings show the grid independence. To ensure calculation accuracy and maintain computational efficiency, all the simulation results in this research were calculated using the medium grid.

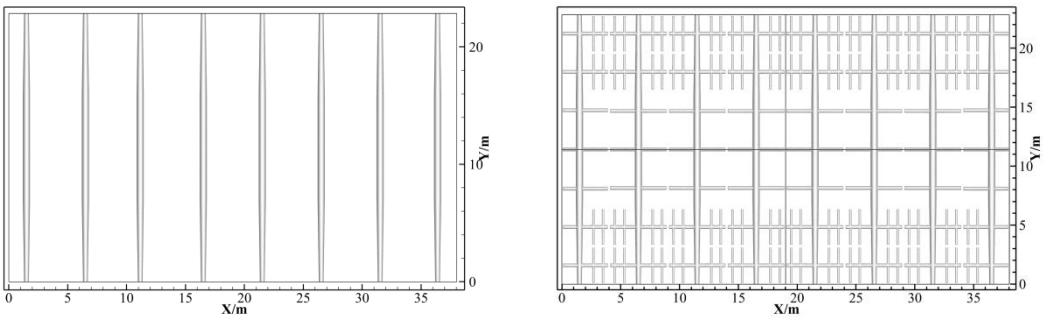

(a) The non-uniform section pipeline

(b) The non-uniform section pipeline incorporated with fractal structure

Fig.2 Physical model of ventilation pipeline distribution

2.2 Numerical model and parameters setting

2.2.1 Numerical model of biomass porous medium

The grain pile in the granary has an elliptical shape, creating interconnected pores between the grains that allow air flow and exchange. This makes the grain pile function as a connected porous medium, with the solid structure formed by accumulated grains. The mechanical ventilation cooling process involves forced convection heat and mass transfer between the porous medium and the cool inlet air. It is important to consider the heat production and humidification resulting from grain biomass respiration and its coupling effect with heat and humidity. To represent the characteristics of the grain pile, sand is chosen as the packing material for the porous medium due to its stable physical properties, non-toxic nature, affordability, large specific heat capacity, cold storage capability, water permeability, and moisture absorption characteristics. The structure of a sand pile resembles that of a grain pile, acting as another connected porous media. Based on theories of heat and mass transfer in porous media, numerical models are developed to simulate the coupled heat and moisture transfer in ventilated grain piles and the heat and mass transfer in ventilated sand piles. Wang et al.[19] compiled previous theories and proposed mathematical formulas (Eq. (1)-(4)) to describe the heat and moisture transfer mechanisms in these systems.

$$\frac{\partial(\varepsilon\rho_a)}{\partial t} + \nabla(\rho_a\vec{u}) = 0 \tag{1}$$

$$\frac{\partial\vec{u}}{\partial t} + (\vec{u}\cdot\nabla)\vec{u} = -\frac{\nabla P}{\rho_a} + \nabla\cdot\left(\frac{\mu}{\rho_a}\nabla\vec{u}\right) + S_m \tag{2}$$

$$\left(\rho_a\varepsilon c_a + \rho_g(1-\varepsilon)c_g\right)\frac{\partial T}{\partial t} + c_a\nabla\cdot(\rho_a\vec{u}T) = K_{eff}\nabla^2 T + S_h \tag{3}$$

$$\frac{\partial(\varepsilon\rho_a w)}{\partial t} + \nabla\cdot(\rho_a\vec{u}w) = \nabla\cdot\left(\rho_a D_{eff}\nabla w\right) + S_w \tag{4}$$

In which, Eq. (1) is the continuity equation, Eq. (2) is the momentum equation, Eq. (3) is the

energy conservation equation, Eq. (4) is the moisture conservation equation. Based on this numerical model, the study analyzes and compares the forced ventilation effects of the two ventilation systems by using FLUENT simulation software.

2.2.2 Numerical model of fractal channel structure optimization in porous medium

When the permeability of porous medium reaches the order of 10^{-3} m^2, the fluid penetration resistance in the medium becomes weak. At a permeability of 1×10^{-2} m^2, the temperature and velocity fields, as well as the streamline in the porous medium, become similar to those observed in pure fluids. Under these conditions, the porous medium can be considered as a space filled with pure fluid[19]. Therefore, in the fractal optimization calculations, the air permeability value in fractal pipelines can be assumed to be 1×10^{-2} m^2. In this particular research, the term "ventilation fractal structure" refers to a composite medium that incorporates the fractal structure proposed by Bejan et al.[15,17,21], which minimizes flow resistance. The minimum pressure drop mathematical model proposed by Bejan et al.[15] is selected as the fractal structure optimization model in this study.

The geometric parameters of the optimized fractals are obtained, as shown in Tab.1.

Table1 Geometric parameters of minimum flow resistance fractal element with unrestricted channel permeability

i	H_i/L_i	$\tilde{H}_i$	$\tilde{L}_i$	$\Delta\tilde{P}_i$
0	$2{C_0}^{-1/2}$	$2^{1/2}{C_0}^{-1/4}$	$2^{-1/2}{C_0}^{1/4}$	$1/2{C_0}^{-1/2}$
1	$(2C_0/C_1)^{1/2}$	$2^{1/2}{C_0}^{1/4}$	${C_0}^{-1/4}{C_1}^{1/2}$	$(2C_0C_1)^{-1/2}$
2	$(2C_1/C_2)^{1/2}$	$2{C_0}^{-1/4}{C_1}^{1/2}$	$2^{1/2}{C_0}^{-1/4}{C_2}^{1/2}$	$(2C_1C_2)^{-1/2}$
$i\geq2$	$(2C_{i-1}/C_i)^{1/2}$	$2^{i/2}{C_0}^{-1/4}{C_{i-1}}^{1/2}$	$2^{(i-1)/2}{C_0}^{-1/4}{C_i}^{1/2}$	$(2C_{i-1}C_i)^{-1/2}$

In this model, the height $\tilde{H}_i$, width $\tilde{L}_i$, and minimum pressure drop $\Delta\tilde{P}_i$ of the rectangular unit are defined as the characteristics of the i-order fractal unit under the minimum pressure loss.

When the channel sizes are small enough, the permeability can be obtained according to the other paper of Bejan et al.[22].

Table2 Geometric parameters of fractal elements

	Height/H (m)	Length/L (m)	Channel Diameter/D (m)
Main pipeline elements	5	22.86	0.4-0.6
First-order fractal elements	3.2	5	0.3
Second-order fractal elements	0.8	3.2	0.15
Minimum fractal elements	0.0044	0.8	0.00022

Note: 1. The minimum fractal unit can be omitted in the fractal structure as its channel diameter size is similar to the sand pore; 2. The height and width of the main pipeline unit are consistent with the size of the non-fractal ventilation system, not the fractal optimization size.

2.2.3 Numerical simulation parameters setting

The grain species is corn. The porosity ε_c of the grain is 0.48, the density ρ_c is 580 [kg • m^{-3}], the permeability K_c is 2.45 × 10^{-8} m^2, and the specific heat capacity C_c of the corn is (1269+34.89M) [$J\cdot kg^{-1}\cdot K^{-1}$)]. The packing of the ventilation zone is sand. The porosity of the sand ε_s is 0.43, the density ρ_s is 1513 [$kg\cdot m^{-3}$], the permeability K_s is 3.69×10^{-9} m^2, the grain pile zone has a constant

internal heat source S_h, the value is 0.01946 [J·m^{-3}], and the specific heat capacity of the sand is C_s = 800 [J·kg^{-1}·K^{-1})]. The geometric parameters of the fractal elements are shown in Tab.3. The initial temperature of the granary is 300 K. This study focuses on the effect of ventilation system on the different of velocity and temperature field in the granary. The boundary conditions are simplified, the thickness of the warehouse wall is 0.2 m, the ambient temperature and the temperature of the outside wall of the warehouse and roof both are set to 298.15 K, the ground temperature is constant to 294.15 K, and all boundary is set to impermeable non-slip boundary conditions. The ventilation system adopts non-fractal ventilation system and fractal ventilation system for cooling ventilation. The ventilation volume per unit (one ton of grain) is 10 [m^3·t^{-1}·h^{-1})], and the ventilation time is 7.5 days (180 hours). The simulation conditions set the non-uniform section pipeline orifice as air inlet, in which the cooling inlet-air is constant temperature and humidity, and the inlet-air temperature is 293 K. Six 2×2 m windows are set up in the front and rear of the warehouse wall above the grain pile as the air outlet, and the outlet pressure is the atmospheric pressure. Due to the complex structure of the fractal ventilation model and the excessive number of geometric grids, for reducing the calculation cost, the fractal ventilation system calculation adopts symmetrical simplification.

2.3 Validation of numerical model

To ensure the accuracy and reliability of the simulation results, the numerical model has been validated by comparing its simulated values with the experimental data from Wang's study[23]. This verification process helps to assess the consistency between the simulation curve and the literature curve. The verification result, as depicted in Fig.3, indicates a strong agreement between the two curves, with consistent trends and high coincidence. The maximum error observed does not exceed 2 °C, indicating that the model exhibits high accuracy and the calculated results are reliable.

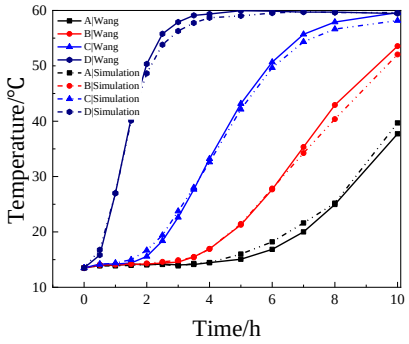

Fig.3 Comparison between simulation value and literature value

Note: Case A, B, C and D represent the literature values[23] and the simulation values of the wheat granary at the heights of 100mm, 260mm, 420mm and 560mm, respectively.

3 Analysis of simulation results

This study focuses on analyzing and comparing the ventilation velocity distribution and temperature distribution in different directions of the granary. The goal is to understand the impact of ventilation velocity on temperature distribution, particularly in terms of uniformity. Average velocity and temperature data for each section of the simulation record are plotted using ORIGIN software.

These line charts facilitate a comprehensive analysis and comparison of the ventilation characteristics between the non-fractal and fractal ventilation systems. The fractal ventilation system diagrams are symmetrically expanded to provide a complete representation.

3.1 Analysis of granary velocity field

The ventilation quality of the non-fractal ventilation system and fractal ventilation system in the granary is analyzed in this research. Three sections in the longitudinal directions are considered. The velocity fields of both systems reach stability after approximately 2 hours for the non-fractal ventilation system and around 45 hours for the fractal ventilation system. After a ventilation and cooling period of 2.5 days (60 hours), the temperature fields of both systems become fully developed. Therefore, the velocity contours at 2.5 days of ventilation and the corresponding temperature contours are selected for analysis.

Three Y-Z plane velocity contours at X=12.7 m(X-12.7), X=16.5 m(X-16.5), and X=19 m(X-19) is selected for analysis based on the pipeline layout, depicted in Fig.4. These contours correspond to different positions: the left side of the transverse distance between adjacent pipelines, the center of the longitudinal pipeline, and the transverse equidistant vertical plane between two adjacent pipelines. These three sections are chosen because they have varying transverse distances from the nearest pipeline, making them representative of the velocity fields in those areas.

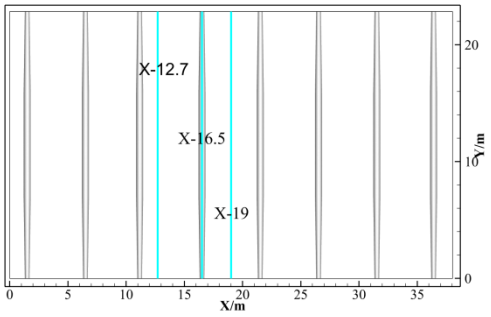

Fig.4 Section of granary

3.1.1 Velocity field of the non-fractal ventilation system

In the non-fractal ventilation system, Fig.5(a) shows that the airflow velocity in each longitudinal section rapidly increases and stabilizes after 2 hours of ventilation. The X-16.5 surface, being the central vertical surface of the pipelines, is most influenced by the pipeline ventilation, resulting in a significantly higher average velocity compared to the other two surfaces. The X-12.7 surface has a slightly higher average velocity than the X-19 surface due to differences in the packing distances through which the ventilation reaches these surfaces. The flow resistance of the porous medium packing is substantial, leading to a significant velocity drop near the channel. However, once the velocity drops to a certain level, the velocity drop becomes less pronounced.

On the X-12.7 surface, the velocity distribution in the grain pile appears relatively uniform, with higher velocities in the middle and lower velocities on the sides. There are areas of weak airflow below on both sides, which may result in poor ventilation in those regions. Additionally, air near the top of the granary accumulates near the side walls and flows towards the windows. On the X-16.5

surface, the velocity near the pipelines is high, but the ventilation velocity in the grain pile at the interface with the packing zone is significantly reduced. This reduction is due to the inconsistent pore structure between the two porous media at the interface, resulting in increased flow resistance in those areas. The iso-velocity lines exhibit a fault at the interface, while the velocity distribution in the remaining positions is similar to that of the X-12.7 surface. Air accumulation occurs near the windows on the top of the granary, leading to an increased velocity on both sides above. For the X-19 surface, the velocity distribution in the grain pile follows a similar pattern to that of the X-12.7 surface, with higher velocities in the middle and lower velocities on the sides. However, the velocity in the center of the packing zone and the local area below on both sides is less than 0.03 [$m \cdot s^{-1}$]. This is because the X-19 surface is a transverse equidistant surface between two ventilation main pipelines, resulting in an offsetting of transverse velocities on this surface. The primary velocity in the packing zone is the transverse velocity, resulting in weaker velocities in those areas. From Fig.5, it can be observed that due to the elevation of the grain pile by the packing zone, there are no areas of poor ventilation within the grain pile. This effectively improves the ventilation quality within the grain pile. Additionally, the discontinuous pore structure at the interface between the sand and the grain pile increases the flow resistance, significantly reducing the velocity of high-velocity ventilation entering the grain pile. This reduction in velocity enhances the uniformity of ventilation at the same height within the grain pile, particularly in regions with weak ventilation in the packing zone.

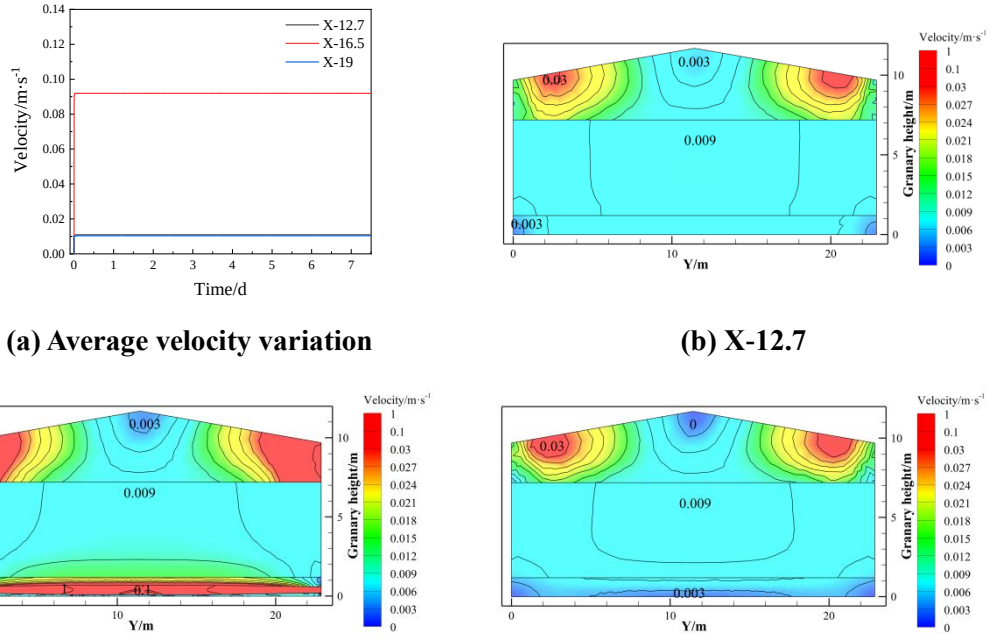

(a) Average velocity variation **(b) X-12.7**

(c) X-16.5 **(d) X-19**

Fig.5 Velocity distribution of non-fractal ventilation system

3.1.2 Velocity field of the fractal ventilation system

In the fractal ventilation system, the Y-Z plane velocity contours at X=12.7, X=16.5, and X=19 are also analyzed. Fig.6(a) demonstrates that due to the complexity of the fractal channel, achieving a balanced ventilation is challenging within a short period of time. Consequently, the ventilation speed in the granary of the fractal ventilation system continues to slowly change after the initial surge and

reaches stability after approximately 45 hours. Overall, compared to the non-fractal ventilation system, the velocity in the fractal system is higher. This improvement can be attributed to the efficient inlet air drainage and diffusion provided by the fractal branch pipelines, which enhance the overall ventilation effectiveness of the granary.

The inclusion of fractal branch pipelines strengthens the ventilation effect and improves the overall ventilation quality. On the X-12.7 surface, the velocity on both sides is low, indicating a more uniform distribution of airspeed contours within the grain pile. The weak ventilation areas on the sides are noticeably weakened, resulting in an enhanced ventilation effect throughout the grain pile. On the X-16.5 surface, the area occupied by the contour with a velocity of 0.012 [$m \cdot s^{-1}$] is smaller compared to the non-fractal ventilation system. This indicates that the inlet air from the pipelines is effectively guided and diffused by the fractal pipelines, leading to better airflow distribution. The velocity contour distribution on the X-19 surface is similar to that of the X-12.7 surface. The fractal branch pipelines play a role in suppressing the weak ventilation area in the packing zone below the ventilation pipe. As a result, the ventilation intensity within the grain pile approaches that of the X-12.7 surface. Overall, the fractal ventilation system efficiently channels the inlet air from non-uniform section pipelines to other areas. Compared to the non-fractal ventilation system, it significantly enhances the ventilation quality in the granary.

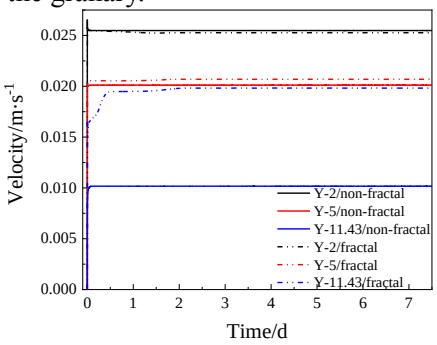

(a) Average velocity variation of longitudinal direction sections

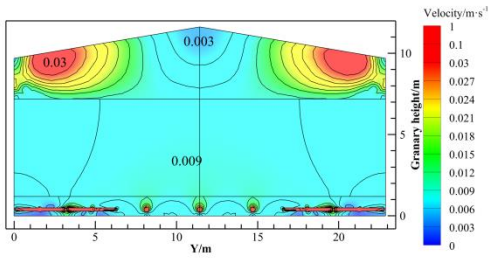

(b) X-12.7

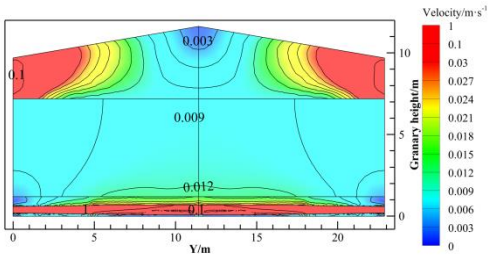

(c) X-16.5

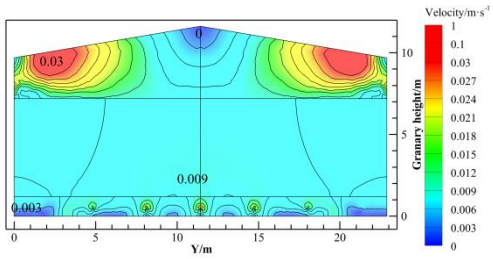

(d) X-19

Fig.6 Velocity distribution of fractal ventilation system

3.2 Temperature field analysis of granary

In order to investigate the impact of velocity field distribution on temperature field variation, this study examines the temperature distribution within the granary at the same surfaces as the velocity contours. After 2.5 days of ventilation, it was observed that the temperature fields in both ventilation systems within the granary had fully developed, and the cold air had reached or permeated the upper

surface of the grain pile. At this point, the overall development of the temperature contours was satisfactory and representative. Therefore, the temperature contours at 2.5 days of ventilation were selected as the focus of analysis.

3.2.1 Temperature field of the non-fractal ventilation system

As depicted in Fig.7(a), the rate of temperature drop in the three curves becomes faster initially, then slows down, and eventually stabilizes. The X-16.5 surface experiences a significant temperature drop at the beginning of ventilation, while the significantly lower temperatures on the X-12.7 surface are delayed by approximately 0.5 days. The X-19 surface exhibits a notable temperature drop in the average temperature curve after around 1.5 days of ventilation. By referring to the non-fractal velocity field contours in Fig.5, it can be observed that the ventilation intensity is strongest on the X-16.5 surface, followed by the X-12.7 surface, and finally the X-19 surface. The cooling rate on these surfaces aligns with their respective ventilation intensities.

The temperature fields of the X-12.7 surface and X-16.5 surface exhibit similarities. The cold front reaches the upper surface of the grain pile, and the isolines are densely distributed in an inverted U-shape. This indicates high ventilation velocity and a high cooling rate on these two surfaces. However, there is poor cooling in the near-wall areas on both sides. In contrast, the isolines on the X-19 surface are sparsely distributed within the grain pile, and the cold front only reaches the middle portion of the grain pile. This differs significantly from the other two surfaces. From Fig. 5(b), it can be observed that the ventilation intensity and airflow on the X-19 surface are weaker. The main direction of ventilation is from bottom to top, lacking direct cooling effects from cold ventilation. As a result, the reduction in temperature on the X-19 surface is limited. Overall, while the cooling effect is good in most areas, there are certain regions that require stronger cooling. These include the near-wall areas on both sides and the middle areas between adjacent pipelines. Additional measures should be taken to strengthen ventilation in these areas.

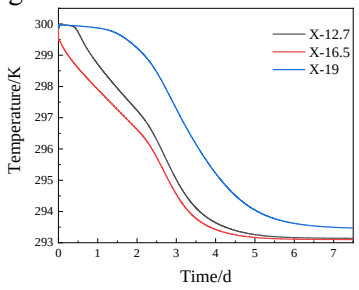

(a) Average temperature variation of longitudinal direction sections

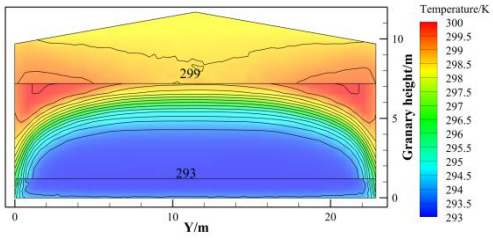

(b)X-12.7

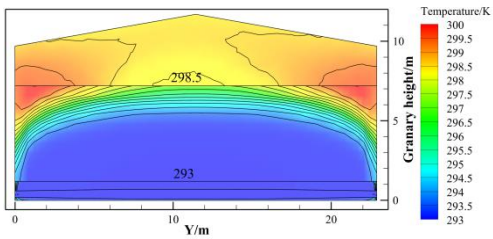

(c)X-16.5

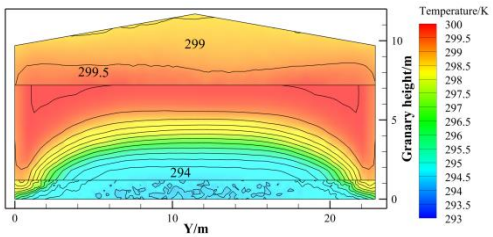

(d)X-19

Fig.7 Temperature distribution of non-fractal ventilation system

3.2.2 Temperature field of the fractal ventilation system

As depicted in Fig.8(a), the longitudinal temperature drop uniformity within the granary is significantly improved in the fractal ventilation system compared to the non-fractal ventilation system. On the X-19 surface and X-12.7 surface, the time at which the temperature drop becomes apparent is greatly advanced, and the average temperature curves of these surfaces are closer together. The average temperature difference between the X-19 surface and X-16.5 surface is effectively reduced, leading to better overall temperature uniformity across the three surfaces. However, it should be noted that the overall cooling rate of the fractal system is lower than that of the non-fractal system. The average temperature curve of the fractal system reaches the final stable temperature approximately 1 day later than that of the non-fractal system. This can be attributed to several factors. Firstly, the fractal structure diverts the inlet air, reducing the permeation capacity of ventilation in porous medium. Additionally, while the enhanced ventilation in local areas improves ventilation effectiveness, it also reduces the cooling rate of the granary as a whole. Overall, while the fractal ventilation system improves temperature uniformity, it comes at the cost of a slightly slower cooling rate compared to the non-fractal system due to changes in airflow distribution and reduced permeation capacity.

Compared to the non-fractal ventilation system, the fractal ventilation system shows significant improvement in cooling uniformity. The temperature in the near-wall areas on both sides of the X-12.7 and X-19 surfaces decreases significantly, and the cold front on both sides does not lag behind the middle cold front. This indicates better overall cooling uniformity on both sides of the granary. In Fig.5(b), it can be observed that the X-19 surface mainly benefits from ventilation enhancement provided by the second-order fractal units and first-order fractal units. The cooling effect is particularly evident near the branch pipelines. As for the X-16.5 surface, although there are limitations in the change of the temperature field, the cooling rate decreases and the heights of the three cold fronts are similar. Overall, the fractal structure effectively improves the uniformity of longitudinal cooling within the granary and enhances the cooling effect in areas where the initial temperature drop is weaker.

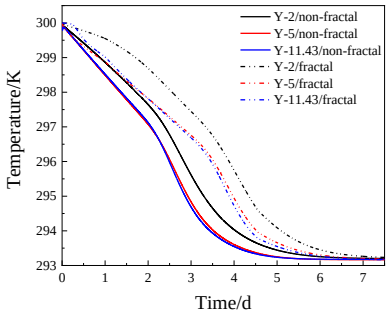

(a) Average temperature variation of longitudinal direction sections

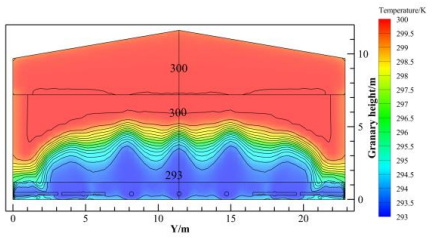

(b)X-12.7

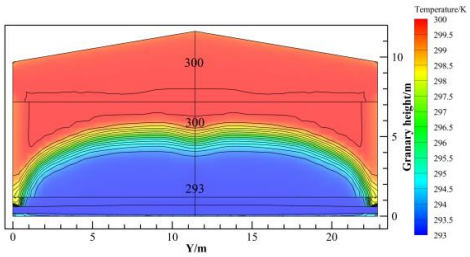

(c)X-16.5

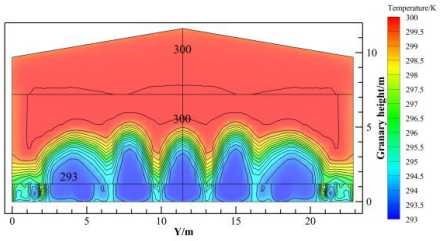

(d)X-19

Fig.8 Temperature distribution of fractal ventilation system

4 Velocity uniformity

To verify the ventilation velocity distribution uniformity in both non-fractal and fractal ventilation systems during ventilation cooling, monitoring points were established at different heights within the grain pile. Seven layers of monitoring points were evenly distributed throughout the pile. The bottom layer was positioned at the base, 1.2 m high, followed by layers at 2 m, 3 m, and so on. The top layer was placed 0.2 m from the upper surface, at a height of 7 m. Each layer had 13 monitoring points, resulting in a total of 91 points in the grain pile. The corner and wall points were spaced 1 m apart, and the rest were uniformly distributed, shown in Fig.9. This layout ensured an appropriate distribution of monitoring points for accurate detection. In the case of the fractal ventilation system, the model was symmetrically expanded to cover the entire system before sampling and counting.

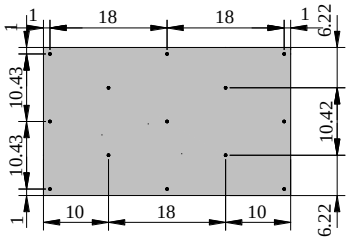

Fig.9 Layout of observation points

To assess the ventilation velocity uniformity in two ventilation systems, different inlet air volumes (10 [$m^3 \cdot t^{-1} \cdot h^{-1}$]) and 15 [$m^3 \cdot t^{-1} \cdot h^{-1}$]) were used to simulate the internal velocity distribution within the grain pile. This allowed for evaluating the uniformity at various heights under different inlet air volumes. The fractal ventilation system's uniformity was also assessed across varying inlet air volumes. By comparing velocity distributions at different heights, a comprehensive evaluation of

velocity uniformity was achieved. For consistency, the grain pile with a ventilation duration of 2.5 days (60 hours) was chosen. The stabilization time for the velocity field varied between the two systems, with one taking around 2 hours and the other approximately 45 hours. Selecting a longer ventilation period ensured a thorough assessment of velocity uniformity, considering the differing stability times of the velocity field.

Weltens et al.[24] proposed the exponent of uniformity (EOU) as a metric to evaluate flow distribution characteristics and represent the uniformity of flow velocity or mixing. In this research, the exponent of uniformity is introduced as a measure to quantify the uniformity of ventilation velocity within grain piles. It serves as the basis for evaluating the uniformity of ventilation velocity in this study. The specific equation for the exponent of uniformity is denoted as Eq. (5).

$$r = 1 - \frac{1}{2n}\sum_{i=1}^{n}\frac{\sqrt{(v_i - \bar{v})^2}}{\bar{v}} \tag{5}$$

In which, r is the exponent of uniformity, which is between 0 and 1. The closer it is to 1, the better the velocity uniformity in the grain pile is. v_i is the velocity of each monitoring point, m·s^{-1}. $\bar{v}$ is the average surface weight velocity of the layer where the monitoring point is located, m·s^{-1}. n is the number of monitoring points.

To evaluate the sampling reliability of monitoring points, the degree of deviation (DOD) is introduced as a reference. The value range is from 0 to 1. The closer it is to 0, the smaller the sampling value deviation is, the higher the reliability is. The calculation formula is Eq. (6).

$$p = \frac{\sqrt{(\bar{v} - \tilde{v})^2}}{\bar{v}} \tag{6}$$

In which, p is the degree of deviation, $\tilde{v} = \frac{1}{n}\sum_{i=1}^{n} v_i$ is the average value of the sum of the sampling velocity of a monitoring layer.

The calculation results are shown in Tab.3.

Table3 Results of grain stack velocity uniformity calculation

	Non-fractal ventilation system				Fractal ventilation system			
Inlet-air per ton of grain ($m^3 \cdot t^{-1} \cdot h^{-1}$)	10		15		10		15	
Height (m)	EOU	DOD	EOU	DOD	EOU	DOD	EOU	DOD
1.2	0.8555	0.0918	0.8152	0.1134	0.8423	0.1247	0.8126	0.1512
2	0.9019	0.0264	0.8812	0.0473	0.8735	0.0885	0.8459	0.1131
3	0.9242	0.0134	0.9034	0.0299	0.9148	0.0787	0.8904	0.0591
4	0.9477	0.0022	0.9336	0.0117	0.9313	0.0296	0.9141	0.0405
5	0.9618	0.0005	0.9520	0.0056	0.9499	0.0180	0.9372	0.0253
6	0.9662	0.0013	0.9576	0.0038	0.9569	0.0141	0.9461	0.0201
7	0.9703	0.0042	0.9627	0.0004	0.9612	0.0115	0.9516	0.0166
Mean	0.9325	0.0200	0.9151	0.0303	0.9185	0.0521	0.8997	0.0608

According to Tab.3, the exponent of uniformity (EOU) for the grain pile is relatively small in the height range from 1.2 m to 2 m, indicating unsatisfactory velocity uniformity within this zone. However, as the height increases beyond 2 m, the EOU noticeably improves, with a minimum value greater than 0.84. This suggests that the velocity uniformity within the zone above 2 m is better, indicating excellent ventilation quality. Although some sampling points are situated above the fractal

branch pipelines, resulting in larger values, which can negatively impact the EOU for the fractal system, the EOU for the fractal ventilation system remains close to that of the non-fractal system under different inlet air volumes. This indicates that the fractal ventilation system maintains good velocity uniformity overall. The average EOU for the fractal system under both inlet air volumes reaches 0.9185 and 0.8997, respectively. The overall deviation level is low. In the fractal system with an inlet air volume of 15 [$m^3 \cdot t^{-1} \cdot h^{-1}$], the maximum deviation degree and maximum average deviation degree are 0.1512 and 0.0608, respectively. These values fall within an acceptable range of error, demonstrating the good reliability of velocity monitoring measurements. These findings suggest that the sampling reliability of velocity monitoring values is high and that the fractal ventilation system maintains satisfactory velocity uniformity.

Conclusion

This research introduced two new ventilation systems: one with porous medium packing around non-uniform section ventilation pipelines, and another incorporating a fractal structure into the non-uniform section pipelines. The goal was to enhance ventilation in areas with lower airflow, improve overall uniformity and quality in the granary. CFD analysis was conducted to compare the velocity and temperature fields of both systems. The research extensively discussed the ventilation and cooling effects by examining the distribution of velocities and temperatures within the grain pile and evaluating velocity uniformity. The findings suggest that:

(1) Sand packing zone can effectively reduce the areas of weak ventilation in grain pile, improve the ventilation quality. The fractal structure in the fractal ventilation system improves airflow by dividing the main pipeline's inlet air, reducing resistance and enhancing airflow in weaker areas. However, this improvement sacrifices the upward penetration rate and rapid diffusion ability. Although the fractal ventilation system achieves better uniformity within the granary, it may not penetrate and diffuse as quickly as the non-fractal system.

(2) In the non-fractal ventilation system, the temperature drop near the inlet and junction area is slow during a 2.5-days ventilation period, resulting in limited cooling. However, above and near the pipelines, the cooling rate is faster, causing significant temperature reduction. This indicates unsatisfactory temperature uniformity within the granary. On the other hand, the fractal ventilation system effectively improves cooling in weak areas where the non-fractal system struggles. Although the overall cooling rate may be slightly slower in the fractal system, it excels in achieving vertical temperature uniformity. The fractal structure significantly enhances cooling uniformity within the granary, addressing previous issues observed in the non-fractal system.

(3) The fractal structure in the ventilation system may have a slight impact on EOU and DOD compared to non-fractal systems. However, data analysis indicates good credibility and suggests that the velocity uniformity in the fractal system is satisfactory. The fractal ventilation system maintains a high level of velocity uniformity and can be considered reliable for practical purposes.

Nomenclature

Variables		$\bar{v}$	Average surface weight velocity, [m·s^{-1}]
c_a	Specific heat capacity of air, [J·kg^{-1}·K^{-1}]	$\tilde{v}$	Average sampling velocity, [m·s^{-1}]
c_g	Specific heat capacity of grain, [J·kg^{-1}·K^{-1}]	v_i	Sampling velocity, [m·s^{-1}]
D_{eff}	Effective diffusion coefficient, [m^2·s^{-1}]	w	Air moisture content, [g • kg^{-1}]
$\widetilde{H}_i$	Height of the i-order fractal unit, [mm]	**Greek symbols**	
i	Order of fractal unit, [-]	∇	Hamiltonian operator/ Del operator
K_{eff}	Effective thermal conductivity, [W·m^{-1}·K^{-1}]	∂	Partial derivative operator
$\tilde{L}_i$	Width of the i-order fractal unit, [mm]	ε	Porosity, [%]
n	Number of monitoring points, [-]	ρ_a	Density of air, [kg·m^{-3}]
p	Degree of deviation, [-]	ρ_g	Density of grain, [kg·m^{-3}]
P	Pressure, [g·m^{-2}]	μ	Viscosity, [kg·s·m^{-1}]
$\Delta\tilde{P}_i$	Minimum pressure loss of the i-order fractal unit, [g·m^{-2}]	**Subscript symbols**	
r	Exponent of uniformity, [-]	a	Air
S_h	Heat source term, [J·m^{-3}·s^{-1}]	eff	Effective coefficient
S_w	Water vapor source term, [g·m^{-3}·s^{-1}]	g	Grain
S_m	Momentum source, [kg·m^{-2}·s^{-2}]	h	Heat
t	Time, [s]	i	Order of fractal unit
T	Temperature, [K]	m	Momentum coefficient
$\vec{u}$	Air velocity, [m·s^{-1}]	w	Water vapor

Reference

[1]Gao Liwei., Characteristics and Reduction of Potentials of Loss and waste of Major Grains of the Food Supply Chain in China, Chinese Academy of Agricultural Sciences, Ph. D. thesis, Beijing, China, 2019 (in Chinese language).

[2]Cui Jinbo., Population Ecology of Major Stored Product Insect Pests in Large Warehouse, MA.Sc. thesis, South Western University of Finance and Economics, Chongqing, China, 2006 (in Chinese language).

[3]Graham R. Thorpe., On the rate of cooling of aerated food grains, *Biosystems Engineering,* 2022, 222, pp. 106-116

[4]Liu Shuling, Wu Zengqiang., Granary ventilation systems and methods, Chinese Patent: 201510608233.4，2017-03-29 (in Chinese language).

[5]Li Jiabin, Wang Yuancheng, Liu Jiaqi, et al., Simulation Study on the Ventilation Effect of a New Type of Ventilation Network on Room-Type Warehouses, *Science and Technology of Cereals, Oils and Foods.* 2023, 31(1), pp. 189-195 (in Chinese language).

[6]Xiong Disheng., Dewdew formation in grain piles with mechanical ventilation and its prevention, *Food Science and Technology and Economy,* 1999, (4), pp. 25-27 (in Chinese language).

[7] Code for Design of Grain Bungalows, Beijing China Planning Publishing House, https://www.sosoarch.com/guifan/details.aspx?id=260 (in Chinese language).

[8]G. R. Thorpe., The application of computational fluid dynamics codes to simulate heat and moisture transfer in stored grains, *Journal of Stored Products Research,* 2008, 44(1), pp. 21-31

[9]G. R. Thorpe., The modelling and potential applications of a simple solar regenerated grain cooling device, *Postharvest Biology and Technology,* 1998, 13(2), pp. 151-168

[10]Daniela de Carvalho Lopes, et al., Aeration simulation of stored grain under variable air ambient conditions, *Postharvest Biology and Technology,* 2006, 42(1), pp. 115-120

[11]Olatunde Gbenga,Atungulu Griffiths G,Sadaka Sammy., CFD modeling of air flow distribution in rice bin storage system with different grain mass configurations, *Biosystems Engineering,* 2016, 151, pp. 286-297

[12]Xiangxiang Zhang,Hao Zhang,Zhenqing Wang, et al., Research on the temperature field of grain piles in underground grain silos lined with plastic, *Journal of Food Process Engineering,* 2022, 45(3)

[13] Tareq Salameh, Mamdouh El Haj Assad, Muhammad Tawalbeh, et al., Analysis of cooling load on commercial building in UAE climate using building integrated photovoltaic façade system, *Solar Energy*, 2020, 199, pp. 617-629

[14]Chen Lingen, Tian Fenghong, Xiao Qinghua, et al., Constructal entransy dissipation rate minimization for mass transfer based on rectangular element with constant channel, *Journal of Thermal Science and Technology,* 2012, 11(2), pp. 136-141

[15]A. Bejan,M. R. Errera., Deterministic Tree Networks for Fluid Flow: Geometry for Minimal Flow Resistance Between a Volume and One Point, *Fractals -london-,* 1997, 5(4), pp. 685-696

[16]Huijun Feng,Lingen Chen,Zhihui Xie, et al., “Volume-Point” Mass Transfer Constructal Optimization Based on Triangular Element, *Arabian Journal for Science and Engineering,* 2013, 38(2), pp. 365-372

[17]Adrian Bejan., Constructal theory: from thermodynamic and geometric optimization to predicting shape in nature, *Energy Conversion and Management,* 1998, 39(16), pp. 1705-1718

[18]Liu Han., Comby fractal microchannel network for fluid flow in porous media, MA.Sc. thesis, Huazhong University of Science and Technology, Wuhan, China, 2014 (in Chinese language).

[19]Yuancheng Wang,Haifeng Duan,Hao Zhang, et al., Modeling on heat and mass transfer in stored wheat during forced cooling ventilation, *Journal of Thermal Science,* 2010, 19(2), pp. 167-172

[20]Chen Baoming, Liu Fang, Yun Heming., *Natural Convective Heat and Mass Transfer in Porous Media*, Science Press, Beijing, China, 2016 (in Chinese language).

[21]Adrian Bejan., Constructal tree network for fluid flow between a finite-size volume and one source or sink, *Revue Générale De Thermique,* 1997, 36(8), pp. 592-604

[22]Errera M.R，Bejan Adrian., Tree Networks for Flows in Composite Porous Media, *Journal of Porous Media,* 1999

[23]Wang Zhenhua. Numerical Simulation and Experimental Study on Heat and Mass Transfer of Stored Grain Pile, Ph. D. thesis, China Agricultural University, Beijing, China, 2014. (in Chinese language).

[24]H. Weltens,H. Bressler,F. Terres, et al., Optimisation of Catalytic Converter Gas Flow Distribution by CFD Prediction, *International Congress & Exposition,* 1993

Paper submitted: 07.08.2023

Paper revised: 20.09.2023

Paper accepted: 30.09.2023